Co-Planning of Regional Wind Resources-based Ammonia Industry and the Electric Network: A Case Study of Inner Mongolia

Jiarong Li, Jin Lin, *Member, IEEE*, Philipp-Matthias Heuser, Heidi Ursula Heinrichs, Jinyu Xiao, Feng Liu, *Senior Member, IEEE*, Martin Robinius, Yonghua Song, *Fellow, IEEE*, and Detlef Stolten

***Abstract*—Converting wind energy into ammonia (WtA) has been recognized as a promising pathway to produce "green" ammonia compared with traditional coal-based technologies. As the key part of WtA, Power-to-Ammonia (PtA) has great potential to facilitate the usage of wind generation. This paper proposes a co-planning approach for regional wind resources-based ammonia industry and the electric network (EN). To this end, PtA is first modeled as a flexible power load of power systems with spatial and temporal constraints on hydrogen supply chains (HSC). Then a novel co-planning model of WtA and EN is established to optimize the WtA configuration and the EN expansion. An alternating direction method of multipliers (ADMM) based algorithm is introduced to effectively solve this model. Real data of Inner Mongolia Province in China is adopted to verify the effectiveness and significance of the proposed approach. It is shown that the siting and operation flexibility of PtA with HSC can reduce the expansion burden of EN. The co-planning of WtA and EN can significantly enhance wind power utilization and reduce total investment costs. Furthermore, feasibility analysis on WtA in comparison with coal-to-ammonia (CtA) and ultra-high voltage transmission (UHV) provides helpful guidelines for the realization of WtA.**

Manuscript received July 26, 2020; revised November 11, 2020 and April 18, 2021; accepted May 29, 2021. Date of publication July 2, 2021; date of current version December 23, 2021. This work was supported by the International S&T Cooperation Program of China (Efficient Integration of Renewable Energies for Natrual Gas Synthesization by High Temperture Electrolysis Technologies, 2018YFE0106700). Paper no. TPWRS-01262-2020. *(Corresponding author: Jin Lin.)*

Jiarong Li is with the State Key Laboratory of Control and Simulation of Power Systems and Generation Equipment, Department of Electrical Engineering, Tsinghua University, Beijing 100084, China (e-mail: jrli16@mails.tsinghua.edu.cn).

Jin Lin and Feng Liu are with the State Key Laboratory of Control and Simulation of Power Systems and Generation Equipment, Department of Electrical Engineering, Tsinghua University, Beijing 100084, China (e-mail: linjin@tsinghua.edu.cn; lfeng@tsinghua.edu.cn).

Philipp-Matthias Heuser, Heidi Ursula Heinrichs, and Martin Robinius are with the Institute of Energy and Climate Research - Techno-Economic Systems Analysis (IEK-3), Forschungszentrum Jülich GmbH, 52425 Jülich, Germany (e-mail: p.heuser@fz-juelich.de; h.heinrichs@fz-juelich.de; m.robinius@fz-juelich.de).

Detlef Stolten is with the Institute of Energy and Climate Research - Techno-Economic Systems Analysis (IEK-3), Forschungszentrum Jülich GmbH, Jülich 52425, Germany, and also with the Fuel Cells, RWTH University of Aachen, 52062 Aachen, Germany (e-mail: d.stolten@fz-juelich.de).

Jinyu Xiao is with the Global Energy Interconnection Development and Cooperation Organization, Beijing 100031, China (e-mail: jinyu-xiao@geidco.org).

Yonghua Song is with the State Key Laboratory of Internet of Things for Smart City, University of Macau, Taipa, Macau SAR 999078, China (e-mail: yhsong@um.edu.mo).

Color versions of one or more figures in this article are available at https://doi.org/10.1109/TPWRS.2021.3089365.

Digital Object Identifier 10.1109/TPWRS.2021.3089365

***Index Terms*—Wind-to-ammonia (WtA), electric network (EN), load model of power-to-ammonia (PtA), co-planning model, the ADMM algorithm, Inner Mongolia.**

NOMENCLATURE

The main notations in this paper are listed below; other symbols are defined as required.

A. Abbreviations

A	Ammonia
ADMM	Alternating direction method of multipliers
ASR	Ammonia synthesis reactor
CtA	Coal-to-ammonia
EL	Electrolyzer
EN	Electric network
EX	Expenditure
EXC	Exchange cost with the other operator
EXP	Expansion
FLH	Full-load hours
HS	Hydrogen buffer tank
HSC	Hydrogen supply chain
HT	Hydrogen truck trailer
HTN	Hydrogen transportation network
KCL	Kirchhoff's current law
L	Local
LCOE	Levelized cost of electricity
LCOA	Levelized cost of ammonia
PtA	Power-to-ammonia
UHV	Ultra-high voltage transmission
WT	Wind turbine
WtA	Wind-to-ammonia

B. Indicators and Sets

i/j	Indicator of regions/nodes
ij	Indicator of branches
$i \to j$	Indicator of paths
t	Indicator of time intervals
R	Set of regions
$\mathbb{N}$	Set of nodes in the EN
$\mathbb{B}$	Set of branches in the EN
P	Set of paths in the HTN
$\mathbb{T}$	Set of time intervals

C. Variables

a. Operation Variables

E_i	Wind energy generation
$P_{i,t}^{\mathrm{RE}}$	Wind power generation
$P_{i,t}^{\mathrm{EL}}$	Load power of electrolyzers
$P_{i,t}^{\mathrm{L}}$	Power for local ammonia production
$P_{i,t}^{\mathrm{ENS}}/\widehat{P}_{i,t}^{\mathrm{ENS}}$	Power injecting to the EN from source regions in the sub-model of WtA/EN
$P_{i,t}^{\mathrm{END}}/\widehat{P}_{i,t}^{\mathrm{END}}$	Power outflow from the EN in demand regions in the sub-model of WtA/EN
$P_{i,t}^{\mathrm{A}}$	Load power of ammonia synthesis reactors
$P_{i,t}$	Node power of the EN
$\theta_{i,t}$	Power angle of the EN
$P_{ij,t}/\widehat{P}_{ij,t}$	Power flow of existing/candidate lines of the EN
$\boldsymbol{P}_{\mathrm{N}}$	Vector of node power in the EN
$\boldsymbol{P}_{\mathrm{B}}/\widehat{\boldsymbol{P}}_{\mathrm{B}}$	Vector of existing/candidate branch power in EN
$n_{i,t}^{\mathrm{H_2}}$	Hydrogen production rate of electrolyzers
$n_{i,t}^{\mathrm{L}}$	Hydrogen production for local ammonia production
$n_{i,t}^{\mathrm{HTS}}$	Hydrogen production to be transported in source regions
$H_{i\to j,t}$	Quantity of hydrogen transport on the path in the HTN
$\boldsymbol{H}_{\mathrm{B}}/\boldsymbol{H}_{P}$	Vector of the quantity of hydrogen transport on the branch/path in the HTN
$m_{i,t}^{\mathrm{HS}}$	Hydrogen inventory in the buffer tank
$n_{i,t}^{\mathrm{in}}/n_{i,t}^{\mathrm{out}}$	Hydrogen input/output flow rate of the buffer tank
$n_{i,t}^{\mathrm{NH_3}}$	Ammonia production rate

b. Planning Variables

P_i^{RE}	The capacity of wind turbines in the WtA
P_i^{EL}	The capacity of electrolyzers in the WtA
m_i^{HS}	The capacity of hydrogen buffer tanks in the WtA
σ_{ij}	Binary variable for the candidate line in the EN

c. Economic Variables

$LCOE_i$	Levelized cost of electricity
$LCOA_i$	Levelized cost of ammonia

D. Parameters

$P_i^{\mathrm{RE,max}}$	Maximal capacity of wind turbines
$P_i^{\mathrm{EL,max}}$	Maximal capacity of electrolyzers
$m_i^{\mathrm{HS,max}}$	Maximal capacity of hydrogen buffer tanks
a_i/b_i	Parameters of E_i-P_i^{RE}
$\mathbf{A}/\mathbf{B}$	Parameters of the ammonia synthesis reactor
$p_{i,t}^{\mathrm{RE}}$	Typical normalized profile of wind generation
η^{EL}	The energy conversion efficiency of the electrolyzer (60%) [27]
$\eta^{\mathrm{in}}/\eta^{\mathrm{out}}$	The hydrogen flow-in/flow-out efficiency of the hydrogen buffer tank (95%) [27]
$k^{\mathrm{EL,min}}/k^{\mathrm{EL,max}}$	The lower/upper limit of the load power of the electrolyzer (20%/100%) [37]
$k^{\mathrm{A,min}}/k^{\mathrm{A,max}}$	The lower/upper limit of the hydrogen flow rate (70%/100%) [9]
$P_{ij,t}^{\min}/P_{ij,t}^{\max}$	The lower/upper limit of transmission capacity of branches in the EN
$\mathbf{T}_{\mathrm{E}}$	The Node-Branch associate matrix of the EN
$\mathbf{T}_{H}$	The Path-Branch associate matrix of the HTN
$H_{i\to j}^{\max}$	The upper limit of the hydrogen transport capacity on paths in the HTN
x_{ij}	The reactance of branches in the EN
$n_i^{\mathrm{NH_3}}$	Ammonia demand
c^{WC}	The wheeling charge of power transmission via the EN (0.008 €/kWh)
c^{HT}	The unit cost of hydrogen transport via trucks (1 €/100km/kg)
ann	Annuity factor of facilities
fix	The fixed ratio of the operational and maintenance cost to the capital cost
c	The unit cost of facilities
Y	The lifetime of facilities
$Dis_{i\to j}$	Distance between region i and region j

I. Introduction

A. Background and Motivations

IN THE past decades, wind generation has been dramatically increasing worldwide, but the lack of transmission capacity and consumption seriously restricts the exploitation of wind resources. As evaluated by the China Meteorological Administration, the technical potential of wind power in China is 2600 GW [1], which corresponds to approximately 7800 TWh of electricity generation under the assumption of average 3000 full-load hours (FLH) per year [2], [3]. However, by the end of 2019, the installed capacity of wind turbines in China was only 210 GW [4]. On the other hand, the development of traditional hydrogen (H_2) -based chemical industry, especially for the ammonia (NH_3) industry, which is responsible for 1%-2% of global energy consumption and CO_2 emissions [5] and represents the largest hydrogen downstream market in China, has been facing pressure from both high fossil fuels consumption and environmental concerns. In 2015, the coal consumption was approximately 80 Mtce (651 TWh) to produce ammonia in China, where the CO_2 emission was approximately 145 Mt, and the annual growth rate was approximately 4% [6].

To meet the aforementioned challenges, a promising solution is to convert the unexploited wind resources into ammonia (WtA), it can create considerable consumption of wind resources while substitutes fossil fuels in the ammonia industry. Following this idea, the USA has launched the "Renewable Energy to Fuels through Utilisation of Energy-Dense Liquids" (REFUEL) program to develop scalable technology for WtA [7]. The first renewable ammonia plant powered by wind energy has been built in Morris [8]. In addition, demonstration projects of WtA have been launched in Japan and Australia [9].

The WtA process involves two phases: 1) first converting wind energy into power via wind turbines; and then 2) converting power into ammonia (PtA). There are mainly two technical routes, which lead to two different PtA processes as follows. For the first route, the power is converted into hydrogen via electrolyzers, and then the hydrogen into ammonia via Haber-Bosch reaction ($N_2 + 3H_2 \rightleftharpoons 2NH_3$) [10]. As the related key technologies are mature, this route is extensively considered in both academia and the ammonia industry. The other route is established on the electrochemical ammonia synthesis technology [11]. Although it has been initially investigated in renewable energy systems [12], its practicality is still lack. In this regard, this paper concentrates on the first PtA route.

As an interface between power and ammonia production, PtA serves as a new type of power load of power systems. It gives rise to not only renewable energy consumption but also additional flexibility to the power system. On the other hand, the electric network (EN) creates new pathways of energy delivery, which may alleviate the intrinsic spatial and temporal constraints of the ammonia industry and reduce the cost for its construction and operation. Considering such interdependence between power systems and ammonia industries, joint optimal planning from the viewpoint of a broader supply chain turns to be a must. In this context, this paper addresses the co-planning problem for WtA and EN, aiming to shed new light on the power system planning combined with other energy sectors.

B. Literature Review

From the perspective of power systems, load modeling of PtA is first focused. The modeling of PtA in the majority of existing researches is based on the ASPEN platform [13]–[17], with a detailed description of the electrolysis process and ammonia synthesis process on voltage, current, temperature, pressure, enthalpy, etc. Based on this kind of model, [13] compares the ammonia production costs with different kinds of renewable energy and cooling methods of the reactor. [14] compares the energy efficiency of three different renewable energy-based ammonia strategies. [15] studies the exergy analysis and operation optimization of a combined solar and wind energy-based ammonia synthesis system. [16] investigates the energy and exergy efficiency of an integrated wind and PV system for ammonia. And [17] analyzes the operation robustness of the WtA system. The modeling of PtA in the above researches can take the secure operation constraints into consideration. However, this kind of model is too complex so that not suitable for the planning research of power systems.

There is another modeling form of PtA with the simplified energy conversion constraints [18]. This kind of model describes the relationship of power and material flows within the energy conversion process. [18] reports a techno-economic analysis for the WtA and analyzes the composition of the production cost of green ammonia in several north European countries. On this basis, [8], [10] consider the secure operation constraints of the electrolyzer, the hydrogen buffer tank, and the ammonia synthesis reactor described with the lower and upper limits on the load power and gas flow. [8] analyzes the effects of key design parameters including the locations of wind turbines and capacities of facilities on the operation cost of the WtA. [10] studies the green ammonia from solar and wind resources in Chile and Argentina.

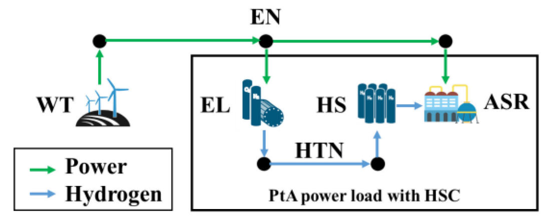

Fig. 1 Illustration of PtA power load with HSC.

Based on the simplified PtA model, there are WtA-related planning researches. [19] studies the capacity planning of electrolyzers and buffer tanks to minimize the investment cost, and [20], [21] determine the optimal planning of renewable ammonia plants.

C. Contributions

With the electrification of the ammonia industry, the PtA plays a key role in the WtA to interconnect the sectors of ammonia industries and power systems. However, existing researches are mainly from the perspective of chemical industries, while limited study has been focusing on the subject from the perspective of power systems. Generally, there are two main gaps in the existing researches:

1) *Load Modeling of PtA:* As shown in Fig. 1, PtA includes two processes, i.e., electrolysis process and ammonia synthesis process. The two processes are linked via a hydrogen buffer tank (HS) [8], [10], [19], which may provide additional operation flexibility to enable a controlled variable load operation of PtA. In addition, the two processes above are not necessarily integrated into the same node of the EN. Instead, they can be connected with the hydrogen transportation network (HTN) [22] in space, as illustrated in Fig. 1, which results in additional siting flexibility for the planning of PtA in power systems. Nevertheless, the benefit of the siting and operation flexibility of PtA for the operation and planning of power systems have seldom been modeled and discussed in the existing literature.
2) *Co-planning of WtA and EN:* As the key part of WtA, the integration of PtA load would definitely request the expansion of EN. On the other hand, the siting and operation flexibility of PtA can facilitate reducing the expansion burden of EN. Therefore, it is desired to coordinate the planning of WtA and EN. However, this interesting problem, to the best of our knowledge, has seldom been explored.

To fill the aforementioned two gaps, this paper addresses the co-planning of regional WtA and EN based on the real data of Inner Mongolia from the perspective of power systems. The main contributions are three-fold:

1) **Modeling level**: PtA is first modeled as a flexible load of power systems with spatial and temporal constraints on hydrogen supply chains (HSC), including hydrogen buffers and hydrogen transport. The security constraints of PtA process are comprehensively considered in this model.
2) **Planning level**: a novel co-planning model of WtA and EN is established to optimize the WtA configuration and the EN expansion. An alternating direction method of multipliers (ADMM) based algorithm is introduced to effectively solve this model, which achieves the minimal total investment while preserving the data privacy of WtA and EN.
3) **Application level**: Inner Mongolia, one of the typical provinces in China with rich wind resources and existing ammonia industries, is selected as the demonstrative example for case studies. Comparative case studies verify the significance of PtA with HSC in reducing the burden of the EN expansion, and the benefit of the co-planning of WtA and EN in facilitating wind power utilization and reducing the total investment cost. Furthermore, insightful feasibility conditions of WtA are provided with a comprehensive comparison with the traditional coal-to-ammonia (CtA) and ultra-high voltage transmission (UHV).

The remainder of the paper is organized as follows: Section II describes the configuration of regional WtA-EN with the actual situations of the unexploited wind resource potential and ammonia industry in Inner Mongolia. Section III proposes the load model of PtA with HSC, and formulates the overall co-planning model of WtA-EN with the ADMM algorithm. In Section IV, the case studies based on an industrial system of Inner Mongolia are performed. Section V concludes the paper.

II. The Generic Configuration of Regional WtA-EN

This section first describes the situation of the unexploited wind resource potential and the ammonia industry in Inner Mongolia in detail. Then, the generic configuration of regional WtA-EN is constructed considering the spatial discrepancy between supply and demand.

A. Wind Resources in Inner Mongolia

Inner Mongolia is a province in the north of China with an area of 1.18 million km^2. It is one of the wind-richest provinces in China with an average wind resource density above 200 W/m^2 and with an existing capacity of wind turbines of 30.07 GW (2019) [23]. However, a great quantity of wind resources remains unexploited according to the following evaluations.

1) The Evaluation Method of Wind Resource Potential: In this paper, we evaluate the wind resources potential of each region in Inner Mongolia based on the method proposed by Ryberg *et al.* [24], [25]. The evaluation flow chart is shown in Fig. 2. First land eligibility evaluation is required, taking sociopolitical, physical, and conservation factors into consideration to determine the eligible land area for wind turbines. Within the eligible land,

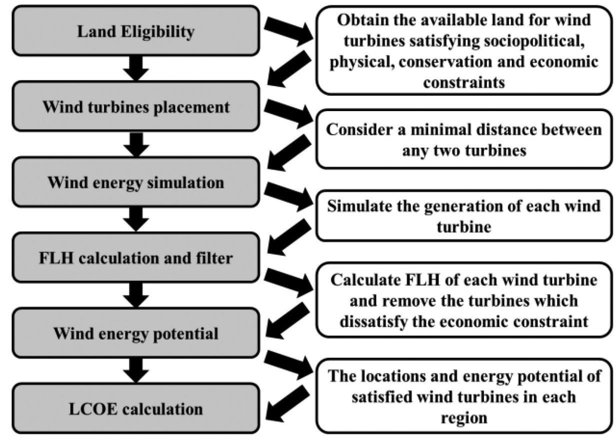

Fig. 2 Flowchart of the evaluation method of wind energy potential.

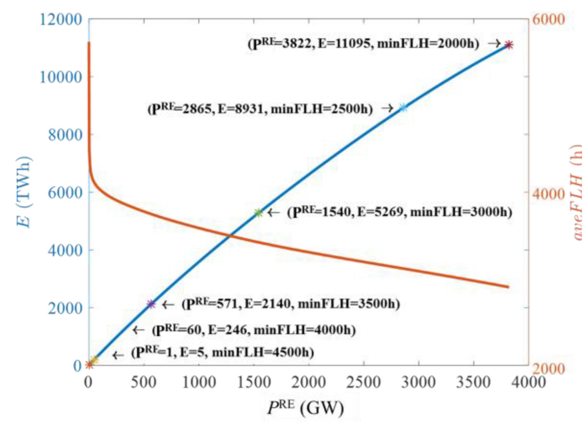

Fig. 3 Evaluation results of wind energy potential in Inner Mongolia.

the wind turbine placement algorithm then determines possible locations of turbines. For those locations, a power curve-based simulation approach is used to derive the FLH for every located turbine. At last, by imposing a minimum permissible FLH (an economic constraint) on this distribution, the number of considered locations along with the energy potential is obtained, which forms the basis to calculate the electricity generation costs.

The evaluation results include the locations and time series output of the satisfied wind turbines, the total wind turbine capacity and wind energy potential in each region can be obtained.

2) Evaluation Results: Fig. 3 shows the relationship of annual wind energy potential E and average FLH with wind turbines' capacity P^{RE} in Inner Mongolia based on the evaluation results. Considering the utilization rate of facilities and total energy required by the ammonia production, the threshold of minimum FLH is set as 4000 h, resulting in a total wind capacity potential of approximately 60 GW with $\sim$246 TWh of annual wind energy in Inner Mongolia.

For simplicity, here, we suppose that the existing wind turbines occupy the best wind resources in each region. The spatial distribution of the remaining unexploited wind turbine capacity potential in Inner Mongolia is shown in Fig. 4. Regions 2 and 11 have the highest unexploited wind resources.

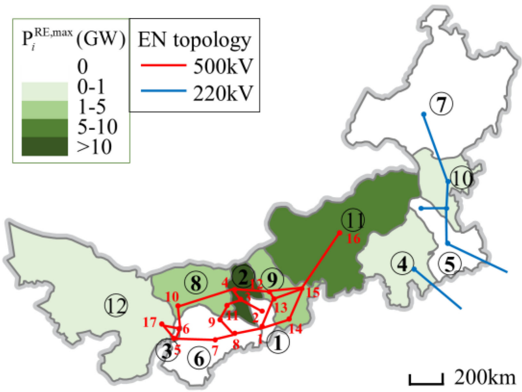

Fig. 4 Distribution of maximal unexploited wind capacity in Inner Mongolia (GW) and the EN topology.

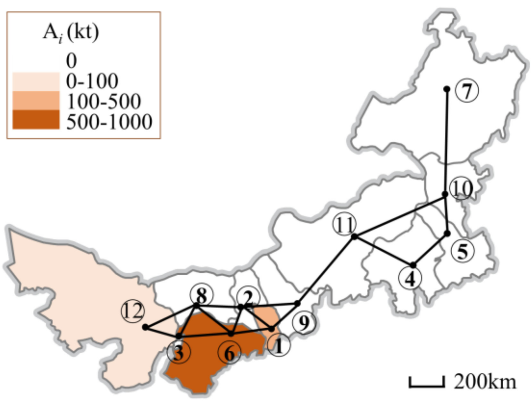

Fig. 5 Distribution of annual ammonia production in Inner Mongolia (kt) and the HTN topology.

B. The Existing Ammonia Industry in Inner Mongolia

Inner Mongolia is one of the major provinces of coal-to-ammonia (CtA) industry in China, with an ammonia production of 1.06 Mt in 2018 [26]. The ammonia industry concentrates on Eerduosi (region 6), Alashan (region 12), and Huhehaote (region 1). Fig. 5 shows the spatial distribution of the ammonia industry in Inner Mongolia.

C. Generic Configuration of Regional WtA-EN

As shown in Figs. 4 and 5, in cases of spatial discrepancies between the wind resource potential and the ammonia industries in Inner Mongolia, a generic configuration of WtA-EN is constructed as shown in Fig. 6. Two types of energy transport modes are considered: power transmission via EN and hydrogen transport via HT (hydrogen truck trailers). Hydrogen pipelines as an alternative hydrogen transportation mode are not considered here as building new hydrogen pipelines might be challenging in Inner Mongolia. Here, we do not consider the ammonia transport mode due to the regulation on ammonia industries, limiting that ammonia production is highly centralized and can only be produced and consumed in regions 1, 6, and 12 in this case study. Regional WtA-EN consists of two independent operators:

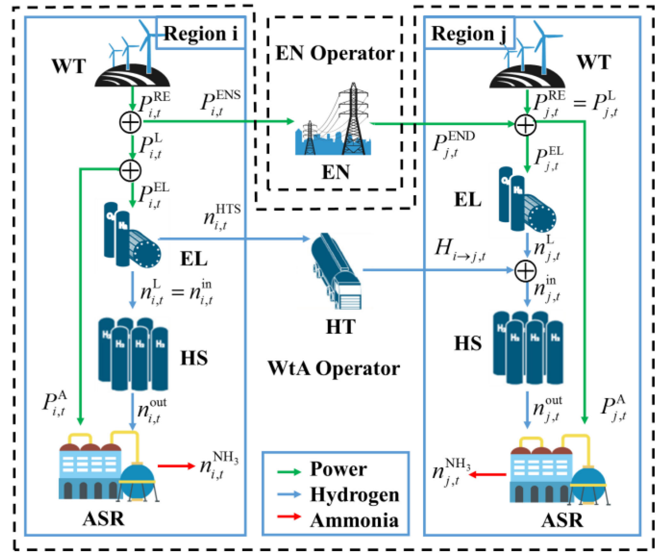

Fig. 6 Illustration of the configuration of regional WtA-EN.

the WtA operator, such as CHN Energy Corporation in Inner Mongolia who is responsible for the investment of wind turbines and ammonia industries; and the EN operator, such as Inner Mongolia Power Corporation or State Grid Corporation who own the EN. The assets ownership of regional WtA-EN is shown in Fig. 6.

Wind resources-based ammonia production means that both power and hydrogen required by ammonia synthesis come from wind energy. The basic process includes:

1) Wind resources are converted into electricity via wind turbines.
2) Wind power $P_{i,t}^{\mathrm{RE}}$ is divided into two parts: one is for power supply for ammonia synthesis process $P_{i,t}^{\mathrm{A}}$, the other is for electrolyzers for hydrogen production $P_{i,t}^{\mathrm{EL}}$.
3) Hydrogen buffer tanks (HS) are required to eliminate the variability of input flow rate $n_{i,t}^{\mathrm{in}}$ from electrolyzers.
4) The hydrogen output from the buffer tanks $n_{i,t}^{\mathrm{out}}$ is converted into ammonia with $P_{i,t}^{\mathrm{A}}$.

By networking the energy transmission, $P_{j,t}^{\mathrm{EL}}$ and $P_{j,t}^{\mathrm{A}}$ can be supplied by both $P_{j,t}^{\mathrm{RE}}$ and power transmission via the EN $P_{j,t}^{\mathrm{END}}$, and $n_{j,t}^{\mathrm{in}}$ can be supplied by both $n_{j,t}^{\mathrm{L}}$ and hydrogen transport via the HTN $H_{i\rightarrow j,t}$, as shown in Fig. 6.

As the key part of WtA, the integration of PtA load would definitely request the expansion of EN. The expansion burden of EN can be potentially reduced by introducing the siting flexibility via HTN and the operation flexibility of PtA via HS. To fulfill this potential, in Section III, the siting and operation flexibility brought by the HSC for PtA load are considered and modeled. On this basis, the co-planning model of WtA and EN is established to optimize the WtA configuration and the EN expansion.

III. Optimal Co-Planning of WtA-EN

In this section, first, for power systems, the load model of PtA with HSC is established. And then, the optimal co-planning model of WtA and EN is proposed. Finally, the distributed ADMM algorithm is presented to solve the proposed co-planning problem.

A. Modeling of PtA With HSC as Flexible Load

From the perspective of power systems, PtA is modeled as a flexible power load with spatial and temporal constraints on HSC. The temporal constraints come from the operation security of each facility, and the spatial constraints come from the process connection of electrolysis and ammonia synthesis via the HTN.

As shown in Fig. 6, the power interconnection of PtA with EN is described as follows:

$$P_{i,t}^{\mathrm{END}} = P_{i,t}^{\mathrm{EL}} - P_{i,t}^{\mathrm{L}} + P_{i,t}^{\mathrm{A}}\ \forall i \in \mathbb{R}, t \in \mathbb{T} \tag{1}$$

where (1) is in a generic form that considers local power generation $P_{i,t}^{\mathrm{L}}$, load power of electrolyzers $P_{i,t}^{\mathrm{EL}}$, and load power of ammonia synthesis reactors $P_{i,t}^{\mathrm{A}}$ together. The internal spatiotemporal constraints on $P_{i,t}^{\mathrm{EL}}$ and $P_{i,t}^{\mathrm{A}}$ are as follows.

1) Operation Constraints of Electrolyzers: The electrolyzer is a kind of energy conversion facility that can convert power $P_{i,t}^{\mathrm{EL}}$ into hydrogen $n_{i,t}^{\mathrm{H_2}}$ described with the conversion efficiency η^{EL} and lower heating value of hydrogen $\mathrm{LHV_{H_2}}$as (2) [27]. Limited by internal operation parameters like current density and temperature, there are lower and upper limits of $P_{i,t}^{\mathrm{EL}}$ to be considered as (3) [28].

$$n_{i,t}^{\mathrm{H_2}} = \frac{P_{i,t}^{\mathrm{EL}}\eta^{\mathrm{EL}}}{\mathrm{LHV_{H_2}}}\ \forall i \in \mathbb{R}, t \in \mathbb{T} \tag{2}$$

$$k^{\mathrm{EL,min}}P_i^{\mathrm{EL}} \le P_{i,t}^{\mathrm{EL}} \le k^{\mathrm{EL,max}}P_i^{\mathrm{EL}}\ \forall i \in \mathbb{R}, t \in \mathbb{T} \tag{3}$$

2) Operation Constraints of Hydrogen Buffer Tanks: Hydrogen buffer tanks are required to balance the fluctuation of the hydrogen flow rate to the acceptable range of the following ammonia synthesis reactor. (4) describes the hydrogen inventory $m_{i,t}^{\mathrm{HS}}$ related to flow-in rate $n_{i,t}^{\mathrm{in}}$ and flow-out rate $n_{i,t}^{\mathrm{out}}$. (5) ensures the hydrogen balance and (6) determines the capacity of m_i^{HS}.

$$m_{i,t}^{\mathrm{HS}} = m_{i,t-1}^{\mathrm{HS}} + n_{i,t}^{\mathrm{in}}\eta^{\mathrm{in}} - n_{i,t}^{\mathrm{out}}/\eta^{\mathrm{out}}\ \forall i \in \mathbb{R}, t \in \mathbb{T} \tag{4}$$

$$m_{i,0}^{\mathrm{HS}} = m_{i,|\mathbb{T}|}^{\mathrm{HS}}\ \forall i \in \mathbb{R} \tag{5}$$

$$m_{i,t}^{\mathrm{HS}} \le m_i^{\mathrm{HS}}\ \forall i \in \mathbb{R}, t \in \mathbb{T} \tag{6}$$

3) Operation Constraints of Ammonia Synthesis Reactors: The ammonia synthesis reactor is a kind of energy conversion facility that can convert hydrogen $n_{i,t}^{\mathrm{out}}$ into ammonia $n_{i,t}^{\mathrm{NH_3}}$ with the power input $P_{i,t}^{\mathrm{A}}$ for auxiliary facilities as (7). Based on our previous research [9], there are lower and upper limits of $n_{i,t}^{\mathrm{out}}$ as (8) due to limits in operation temperature of the catalyst.

$$[n_{i,t}^{\mathrm{NH_3}}, P_{i,t}^{\mathrm{A}}] = \mathbf{A}n_{i,t}^{\mathrm{out}} + \mathbf{B}\ \forall i \in \mathbb{R}, t \in \mathbb{T} \tag{7}$$

$$k^{\mathrm{A,min}}n_i^{\mathrm{NH_3}} \le n_{i,t}^{\mathrm{out}} \le k^{\mathrm{A,max}}n_i^{\mathrm{NH_3}}\ \forall i \in \mathbb{R}, t \in \mathbb{T} \tag{8}$$

where coefficient vectors $\mathbf{A}$ and $\mathbf{B}$ in (7) describe the relationship of $n_{i,t}^{\mathrm{NH_3}}$ and $P_{i,t}^{\mathrm{A}}$ with $n_{i,t}^{\mathrm{out}}$, the detailed coefficients $k^{\mathrm{A,min}}$ and $k^{\mathrm{A,max}}$ are determined by the parameters in [13].

Besides, the ammonia demand should be satisfied as below:

$$\sum_{t=1}^{|\mathbb{T}|} n_{i,t}^{\mathrm{NH_3}} \ge n_i^{\mathrm{NH_3}}\ \forall i \in \mathbb{R} \tag{9}$$

4) Operation Constraints of Hydrogen Transportation: Here, we model the hydrogen transportation network based on the Moore neighborhood model [29], [30]. (10) describes the relationship of paths between any two regions and branches between any adjacent regions based on the shortest route set. The shortest route set is obtained by the Floyd algorithm. $\mathbf{T}_H$ consists of 0 and 1, and 1 means that the branch *ij* belongs to the shortest route set of path *i*→*j*. Note that both branches and paths are directed.

$$\boldsymbol{H}_{\mathrm{B}} = \mathbf{T}_H\boldsymbol{H}_P \tag{10}$$

Considering the maximal traveling distance per day of the truck, hydrogen transportation is not considered on path *i*→*j*, whose shortest distance is larger than the maximal daily traveling distance.

$$H_{i\to j,t} \le H_{i\to j}^{\max}\ \forall i \to j \in \mathbb{P}, t \in \mathbb{T} \tag{11}$$

5) Spatial Constraints of PtA with HTN: The hydrogen interconnection of PtA with HTN shown in Fig. 6 is described as follows:

$$n_{i,t}^{\mathrm{H_2}} = n_{i,t}^{\mathrm{L}} + n_{i,t}^{\mathrm{HTS}}\ \forall i \in \mathbb{R}, t \in \mathbb{T} \tag{12}$$

$$\sum_{t=1}^{|\mathbb{T}|} n_{i,t}^{\mathrm{HTS}} = \sum_{j\in\mathbb{R}}\sum_{t=1}^{|\mathbb{T}|} H_{i\to j,t}\ \forall i \in \mathbb{R}, t \in \mathbb{T} \tag{13}$$

$$n_{i,t}^{\mathrm{in}} = n_{i,t}^{\mathrm{L}} + \sum_{j\in\mathbb{R}} H_{j\to i,t}\ \forall i \in \mathbb{R}, t \in \mathbb{T} \tag{14}$$

where (12), (13), and (14) describe the hydrogen balance at the electrolyzer, during transportation, and at the hydrogen buffer tank, respectively. Notice that the balance constraint during the transportation is in the form of energy balance rather than flow balance since hydrogen trailers are mobile daily storages [31].

B. Co-Planning Model of WtA-EN

The co-planning model of WtA and EN is given by (15). The objective of the co-planning model is to minimize the overall investment and operation costs of WtA and EN. On this basis, the minimum green ammonia production cost can be calculated and then the economic feasibility of WtA can be evaluated.

$$\begin{aligned} &\min EX^{\mathrm{WtA}} + EX^{\mathrm{EN}} \\ &s.t.\ (1)\text{–}(14),\ (16)\text{–}(22),\ (29)\text{–}(37) \end{aligned} \tag{15}$$

where EX^{WtA} represents the investment and operation costs of the WtA operator including the wheeling charge paid for the EN operator, EX^{EN} represents the expansion cost of the EN and the income from the WtA operator. The constraints include the overall planning and operation constraints of WtA (1)–(14), (16)–(22), and EN (29)–(37). The co-planning model of WtA-EN in (15) can be split into two sub-models of WtA and EN with a decomposable structure. The detailed expressions of the two sub-models are as below.

1) The Sub-model of WtA: Based on the PtA load model in (1)–(14), the operation constraints of wind power, the spatial constraints of WtA with EN, the planning constraints of WtA facilities, and the objective function are introduced as below, respectively.

1) Operation Constraints of Wind Power

For unexplored wind resources, there are two important indices related to the utilization cost of wind resources: i) FLH, which is referred to the equivalent annual full-load hours of wind turbines and expressed as $\mathrm{FLH} = \sum_{t=1}^{8760} P_{i,t}^{\mathrm{RE}}/P_i^{\mathrm{RE}}$ [32]. FLH is a general index to reflect the levelized cost of electricity (LCOE), which strongly impacts the levelized cost of ammonia (LCOA) as discussed in case studies; ii) Variability, which influences the utilization rate of following facilities in the WtA process chain such as electrolyzers and hydrogen buffer tanks [10], and influences the levelized cost of ammonia (LCOA).

a) Constraint Related to FLH

For unexplored wind resources, the average FLH of wind turbines decreases with the increasing P_i^{RE}. This phenomenon is shown in Fig. 3 and verified in [32] since the wind turbines with higher FLH should be established first. Based on the evaluation results of wind resources in each region, the relationship of E_i with P_i^{RE} in region *i* can be described by fitting with the quadratic function in (16).

$$E_i \le a_i P_i^{\mathrm{RE}^2} + b_i P_i^{\mathrm{RE}}\ \forall i \in \mathbb{R} \tag{16}$$

b) Constraint Related to Variability

Based on the evaluation results of wind resources in region *i*, we can obtain the simulation profile of each turbine. To describe the nonlinear relationship of $P_{i,t}^{\mathrm{RE}}$ with P_i^{RE} considering the decline tendency of average FLH and ensure that $P_{i,t}^{\mathrm{RE}} \le P_i^{\mathrm{RE}}$ always holds, the normalized profile $p_{i,t}^{\mathrm{RE}} = p_{i,t}^{\mathrm{RE},k} = P_{i,t}^{\mathrm{RE},k}/E_i^k$ of the turbine *k* with the highest FLH is chosen to represent the typical profile in region *i*. Therefore, wind power $P_{i,t}^{\mathrm{RE}}$ can be described by (17).

$$P_{i,t}^{\mathrm{RE}} = E_i p_{i,t}^{\mathrm{RE}}\ \forall i \in \mathbb{R}, t \in \mathbb{T} \tag{17}$$

2) Spatial Constraints of WtA with EN

(1) describes the interconnection of PtA with EN, as shown in Fig. 6, the power interconnection of wind turbines with EN is described as (18).

$$P_{i,t}^{\mathrm{ENS}} = P_{i,t}^{\mathrm{RE}} - P_{i,t}^{\mathrm{L}}\ \forall i \in \mathbb{R}, t \in \mathbb{T} \tag{18}$$

The power balance constraint of the interconnection of WtA with EN is given by (19).

$$\sum_{i \in \mathbb{R}} P_{i,t}^{\mathrm{ENS}} - P_{i,t}^{\mathrm{END}} = 0\ \forall t \in \mathbb{T} \tag{19}$$

3) Upper Limits on the Capacity of WtA Facilities

The configuration of WtA requires new planning for related facilities, including wind turbines, electrolyzers, and hydrogen buffer tanks. Considering the wind resources and land eligibility, there are upper limits in each region as (20)–(22).

$$P_i^{\mathrm{RE}} \le P_i^{\mathrm{RE,max}}\ \forall i \in \mathbb{R} \tag{20}$$

$$P_i^{\mathrm{EL}} \le P_i^{\mathrm{EL,max}}\ \forall i \in \mathbb{R} \tag{21}$$

$$m_i^{\mathrm{HS}} \le m_i^{\mathrm{HS,max}}\ \forall i \in \mathbb{R} \tag{22}$$

4) Objective Function

For the WtA operator, the overall expense of the WtA configuration EX^{WtA} can be divided into two components: one is an internal cost from wind turbines EX_i^{RE}, electrolyzers EX_i^{EL}, hydrogen buffer tanks EX_i^{HS}, and hydrogen transportation $EX_{i\to j}^{\mathrm{HT}}$, the other is an external cost which is the exchange cost with the EN operator EX_i^{EXC}. The general calculation method of cost in (24)–(26), (39) for facilities is obtained from Heuser *et al.* [32].

$$\begin{aligned}\min EX^{\mathrm{WtA}} = &\underbrace{\sum_{i\in\mathbb{R}} EX_i^{\mathrm{RE}} + EX_i^{\mathrm{EL}} + EX_i^{\mathrm{HS}} + \sum_{i\to j\in\mathbb{P}} EX_{i\to j}^{\mathrm{HT}}}_{\text{internal}}\\ &+ \underbrace{\sum_{i\in\mathbb{R}} EX_i^{\mathrm{EXC}}}_{\text{external}}\end{aligned} \tag{23}$$

$$EX_i^{\mathrm{RE}} = \mathrm{ann}^{\mathrm{RE}}(c^{\mathrm{RE}} P_i^{\mathrm{RE}}(1 + \mathrm{fix}^{\mathrm{RE}})) \tag{24}$$

$$EX_i^{\mathrm{EL}} = \mathrm{ann}^{\mathrm{EL}}(c^{\mathrm{EL}} P_i^{\mathrm{EL}}(1 + \mathrm{fix}^{\mathrm{EL}})) \tag{25}$$

$$EX_i^{\mathrm{HS}} = \mathrm{ann}^{\mathrm{HS}}(c^{\mathrm{HS}} m_i^{\mathrm{HS}}(1 + \mathrm{fix}^{\mathrm{HS}})) \tag{26}$$

$$EX_{i\to j}^{\mathrm{HT}} = \sum_{t=1}^{|\mathbb{T}|} c^{\mathrm{HT}} Dis_{i\to j} H_{i\to j,t} \tag{27}$$

$$EX_i^{\mathrm{EXC}} = \sum_{t=1}^{|\mathbb{T}|} c^{\mathrm{WC}} P_{i,t}^{\mathrm{END}} \tag{28}$$

where $\mathrm{ann} = \frac{(1+r)^{\mathrm{Y}} r}{(1+r)^{\mathrm{Y}} - 1}$ is the annuity factor, Y is the lifetime of facilities and $r = 8\%$ is the annual interest rate. Notice that following the above calculation method, EX^{WtA} represents the annual cost. (27) represents the hydrogen transport cost via HT related to the investment, operation and maintenance costs for trucks and trailers. (28) represents the power transmission cost via the EN related to the fixed wheeling charge.

In summary, the sub-model of regional WtA includes the objective shown in (23)–(28) and the constraints shown in (1)–(14), (16)–(22).

a) The Sub-model of EN

The sub-model of EN determines the optimal expansion of transmission lines with satisfying the power flow operation constraints, and planning limits on the number of candidate lines. The detailed expressions of the constraints and the objective function are introduced as below, respectively.

1) Operation Constraints of EN

Based on the DC flow model [33], the power flow of the existing line $P_{ij,t}$ can be described as (29), and the power flow of the candidate line $\widehat{P}_{ij,t}$ can be described as (30) based on the classic disjunctive model [34]:

$$P_{ij,t} = (\theta_{i,t} - \theta_{j,t})/x_{ij}\ \forall i,j \in \mathbb{N}, ij \in \mathbb{B}, t \in \mathbb{T} \tag{29}$$

$$|\widehat{P}_{ij,t} - (\theta_{i,t} - \theta_{j,t})/x_{ij}| \leq M(1 - \sigma_{ij}) \; \forall i, j \in \mathbb{N}, ij \in \mathbb{B}, t \in \mathbb{T} \tag{30}$$

$$\theta_{\text{ref},t} = 0 \; \forall t \in \mathbb{T} \tag{31}$$

where M represents a big constant in (30). (31) is the constraint of the power angles with respect to the reference node. (32)–(33) show the lower and upper limits of the line flows.

$$P_{ij}^{\min} \leq P_{ij,t} \leq P_{ij}^{\max} \; \forall ij \in \mathbb{B}, t \in \mathbb{T} \tag{32}$$

$$P_{ij}^{\min}\sigma_{ij} \leq \widehat{P}_{ij,t} \leq P_{ij}^{\max}\sigma_{ij} \; \forall ij \in \mathbb{B}, t \in \mathbb{T} \tag{33}$$

Kirchhoff's Current Law (KCL) constraint of each node should be satisfied, which means that $P_{i,t}$ from node *i* should be equal to the sum of $P_{ij,t}$ and $\widehat{P}_{ij,t}$ of branch *ij* where node *j* is adjacent to node *i*. It can be described with the node-branch associate matrix $\mathbf{T}_{\text{E}}$ as (34), which describes the topology of the EN and establishes the relationship of nodes and branches.

$$\boldsymbol{P}_{\text{N}} = \mathbf{T}_{\text{E}}(\boldsymbol{P}_{\text{B}} + \widehat{\boldsymbol{P}}_{\text{B}}) \tag{34}$$

The power balance of the electric network is depicted in (35).

$$\sum_{i \in \mathbb{N}} P_{i,t} = 0 \; \forall t \in \mathbb{T} \tag{35}$$

In the sub-model of EN, two auxiliary variables $\widehat{P}_{i,t}^{\text{ENS}}$ and $\widehat{P}_{i,t}^{\text{END}}$ are considered to be the same as $P_{i,t}^{\text{ENS}}$ and $P_{i,t}^{\text{END}}$ in the sub-model of WtA, and (36) defines the relationship of $P_{i,t}$ with WtA.

$$P_{i,t} = \begin{cases} \widehat{P}_{i,t}^{\text{ENS}} - \widehat{P}_{i,t}^{\text{END}}, i \in \mathbb{R} \\ 0, i \in \mathbb{N} \backslash \mathbb{R} \end{cases} \; \forall t \in \mathbb{T} \tag{36}$$

2) Upper Limits on the Number of Candidate Lines

The number of transmission lines for expansion in the EN should not exceed the upper limit for branch *ij* as (37).

$$\sigma_{ij} \leq \sigma_{ij}^{\max} \; \forall ij \in \mathbb{B} \tag{37}$$

3) Objective Function

For the EN operator, the overall expense EX^{EN} can be divided into two components, as shown in (38). One is an internal cost from the expansion of transmission lines EX_{ij}^{EXP}, the other is an external cost that represents the income from the WtA operator EX_i^{EXC}. EX^{EN} also represents the annual cost.

$$\min EX^{\text{EN}} = \underbrace{\sum_{ij \in \mathbb{B}} EX_{ij}^{\text{EXP}}}_{\text{internal}} - \underbrace{\sum_{i \in \mathbb{R}} EX_i^{\text{EXC}}}_{\text{external}} \tag{38}$$

$$EX_{ij}^{\text{EXP}} = \text{ann}^{\text{EXP}}(c_{ij}^{\text{EXP}}\sigma_{ij}(1 + \text{fix}^{\text{EXP}})) \tag{39}$$

$$EX_i^{\text{EXC}} = \sum_{t=1}^{|\mathbb{T}|} c^{\text{WC}} \widehat{P}_{i,t}^{\text{END}} \tag{40}$$

In summary, the sub-model of EN includes the objective shown in (38)–(40) and the constraints shown in (29)–(37).

C. Calculation Methods of Economic Indices

1) LCOE: $LCOE_i$ of region *i* is defined as the levelized electricity generation cost, which is related to the cost from wind turbines and calculated as (41).

$$LCOE_i = \frac{EX_i^{\text{RE}}}{\sum_{t=1}^{|\mathbb{T}|} P_{i,t}^{\text{RE}}} \; \forall i \in \mathbb{R} \tag{41}$$

2) LCOA: $LCOA_i$ of region *i* is defined as the levelized ammonia generation cost, which is related to the overall cost of WtA and calculated as (42).

$$LCOA_i = \frac{EX_i^{\text{WtA}}}{\sum_{t=1}^{|\mathbb{T}|} n_{i,t}^{\text{NH}_3}} \; \forall i \in \mathbb{R} \tag{42}$$

D. An ADMM-Based Solution Approach

The co-planning of WtA and EN consists of two independent operators: the WtA operator and the EN operator. The ADMM algorithm is suitable for solving this kind of co-planning problem with independent operators, which help preserve the data privacy of each operator while achieving the benefits of the co-planning. Its effectiveness has been verified in network co-planning research [35].

The wheeling charge EX_i^{EXC} paid for the EN operator by the WtA operator is in the objective function of each operator. And the coupling constraints between WtA sub-model and EN sub-model are (43)–(44):

$$P_{i,t}^{\text{ENS}} = \widehat{P}_{i,t}^{\text{ENS}} \; \forall i \in \mathbb{R}, t \in \mathbb{T} \tag{43}$$

$$P_{i,t}^{\text{END}} = \widehat{P}_{i,t}^{\text{END}} \; \forall i \in \mathbb{R}, t \in \mathbb{T} \tag{44}$$

Under the above preparation, the co-planning model can be reformulated and solved by the conventional ADMM algorithm [36]. The augmented Lagrangian is as below:

$$\begin{aligned} & L_\rho(\boldsymbol{x}, \boldsymbol{z}, \boldsymbol{y}) \\ & = EX^{\text{WtA}}(\boldsymbol{x}) + EX^{\text{EN}}(\boldsymbol{z}) \\ & \quad + (\boldsymbol{y}^1)^{\text{T}}(\boldsymbol{P}^{\text{ENS}} - \widehat{\boldsymbol{P}}^{\text{ENS}}) + (\boldsymbol{y}^2)^{\text{T}}(\boldsymbol{P}^{\text{END}} - \widehat{\boldsymbol{P}}^{\text{END}}) \\ & \quad + (\rho/2)\left[||\boldsymbol{P}^{\text{ENS}} - \widehat{\boldsymbol{P}}^{\text{ENS}}||_2^2 + ||\boldsymbol{P}^{\text{END}} - \widehat{\boldsymbol{P}}^{\text{END}}||_2^2\right] \end{aligned} \tag{45}$$

where ***x*** includes variables determined by WtA sub-model in (1)–(14), (16)–(22), ***z*** includes variables determined by EN sub-model in (29)–(37). ***y*** is the Lagrange multiplier where $\boldsymbol{y}^1$ is the dual variable for constraint (43) and $\boldsymbol{y}^2$ is for (44). ρ is the penalty parameter.

The detailed iterations consist of three key stages as follows. *k* is the iteration time:

Stage 1: Updating x: $\boldsymbol{x}^k \rightarrow \boldsymbol{x}^{k+1}$

Based on the sub-model of WtA, the update of ***x*** is the process of solving the below problem as (46).

$$\begin{aligned}&\min_{\boldsymbol{x}} L_\rho(\boldsymbol{x},\boldsymbol{z}^k,\boldsymbol{y}^k)\\&= EX^{\mathrm{WtA}}(\boldsymbol{x}) + \sum_{i\in\mathbb{R}}\sum_{t=1}^{|\mathbb{T}|}\left[(y_{i,t}^1)^k - \rho(\widehat{P}_{i,t}^{\mathrm{ENS}})^k\right]P_{i,t}^{\mathrm{ENS}}\\&\quad + \left[(y_{i,t}^2)^k - \rho(\widehat{P}_{i,t}^{\mathrm{END}})^k\right]P_{i,t}^{\mathrm{END}}\\&\quad + (\rho/2)\left[(P_{i,t}^{\mathrm{ENS}})^2 + (P_{i,t}^{\mathrm{END}})^2\right]\\&\quad \text{s.t. (1)–(14), (16)–(22)}\end{aligned}\tag{46}$$

Stage 2: Updating z: $z^k \to z^{k+1}$

Based on the sub-model of EN, the update of $\boldsymbol{z}$ is the process of solving the below problem as (47).

$$\begin{aligned}&\min_{\boldsymbol{z}} L_\rho(\boldsymbol{x}^{k+1},\boldsymbol{z},\boldsymbol{y}^k)\\&= EX^{\mathrm{EN}}(\boldsymbol{z}) + \sum_{i\in\mathbb{R}}\sum_{t=1}^{|\mathbb{T}|}\left[-(y_{i,t}^1)^k - \rho(P_{i,t}^{\mathrm{ENS}})^{k+1}\right]\widehat{P}_{i,t}^{\mathrm{ENS}}\\&\quad + \left[-(y_{i,t}^2)^k - \rho(P_{i,t}^{\mathrm{END}})^{k+1}\right]\widehat{P}_{i,t}^{\mathrm{END}}\\&\quad + (\rho/2)\left[(\widehat{P}_{i,t}^{\mathrm{ENS}})^2 + (\widehat{P}_{i,t}^{\mathrm{END}})^2\right]\\&\quad \text{s.t. (29)–(37)}\end{aligned}\tag{47}$$

Stage 3: Updating y: $y^k \to y^{k+1}$

The update of $\boldsymbol{y}$ obeys formulas below:

$$\begin{aligned}(y_{i,t}^1)^{k+1} &= (y_{i,t}^1)^k + \rho\left[(P_{i,t}^{\mathrm{ENS}})^{k+1} - (\widehat{P}_{i,t}^{\mathrm{ENS}})^{k+1}\right]\\(y_{i,t}^2)^{k+1} &= (y_{i,t}^2)^k + \rho\left[(P_{i,t}^{\mathrm{END}})^{k+1} - (\widehat{P}_{i,t}^{\mathrm{END}})^{k+1}\right]\end{aligned}\tag{48}$$

The complete ADMM algorithm for solving this problem also needs the initialization of parameters and the stopping criteria in (49)–(50).

$$\begin{aligned}&||(\boldsymbol{P}^{\mathrm{ENS}})^{k+1} - (\widehat{\boldsymbol{P}}^{\mathrm{ENS}})^{k+1}; (\boldsymbol{P}^{\mathrm{END}})^{k+1} - (\widehat{\boldsymbol{P}}^{\mathrm{END}})^{k+1}||_2\\&\le \varepsilon \max\{||(\boldsymbol{P}^{\mathrm{ENS}})^{k+1};(\boldsymbol{P}^{\mathrm{END}})^{k+1}||_2, ||(\widehat{\boldsymbol{P}}^{\mathrm{ENS}})^{k+1};\\&\qquad (\widehat{\boldsymbol{P}}^{\mathrm{END}})^{k+1}||_2\}\end{aligned}\tag{49}$$

$$\begin{aligned}&||\rho\left[(\widehat{\boldsymbol{P}}^{\mathrm{ENS}})^{k+1} - (\widehat{\boldsymbol{P}}^{\mathrm{ENS}})^{k}\right];\rho\left[(\widehat{\boldsymbol{P}}^{\mathrm{END}})^{k+1} - (\widehat{\boldsymbol{P}}^{\mathrm{END}})^{k}\right]||_2\\&\le \varepsilon||(\boldsymbol{y}^1)^{k+1};(\boldsymbol{y}^2)^{k+1}||_2\end{aligned}\tag{50}$$

where (49) is the stopping criteria for primary residual and (50) is for dual residual. ε is the relative tolerance.

The overall algorithm flowchart is concluded in Table I:

From Table I, Step 1 is the process of solving a QCP (quadratically constrained programming) problem in (46) and Step 2 is the process of solving a MILP (mixed-integer linear programming) problem in (47), above problems can be solved with CPLEX solver. Steps 3 and 4 are algebraic calculations.

TABLE I
THE ADMM ALGORITHM FOR WTA-EN CO-PLANNING MODEL

Initialization: k=0, $\boldsymbol{y}^0$=**1**, ρ =1, $\varepsilon=10^{-3}$, $(\boldsymbol{P}^{\mathrm{ENS}})^0=\boldsymbol{0}$, $(\boldsymbol{P}^{\mathrm{END}})^0=\boldsymbol{0}$
while (49) and (50) = 0, do
Step1: solve (46) and update $\boldsymbol{x}$
Step2: solve (47) and update $\boldsymbol{z}$
Step3: calculate (48) and update $\boldsymbol{y}$
Step4: calculate left and right terms in (49) and (50)
k=k+1
end while

TABLE II
ECONOMIC INDEXES OF FACILITIES

Cost	c	fix	Y (years)
EX^{RE} [38]	1000 €/kW	2%	20
EX^{EL} [27]	375 €/kW	3%	10
EX^{HS} [39]	500 €/kg H_2	2%	20
EX^{EXP}	125 k€/km (617MW,500kV)	5%	40
EX^{UHV}	1. 28.25 billion€ (10GW, ±1000kV) 2. 17.13 billion€ (8GW, ±800kV) 3. 13.63 billion€ (6GW, ±800kV)	5%	40

IV. CASE STUDIES

In this section, case studies are performed using real data from the industrial system of Inner Mongolia. First, the optimal co-planning results of WtA-EN are obtained based on the proposed WtA-EN co-planning model with the ADMM algorithm. And then, four comparative cases are discussed, which reveals the significance of the PtA load with HSC and the co-planning of WtA-EN. Furthermore, key factors related to the siting and sizing of WtA facilities are analyzed. Finally, WtA is quantitatively compared with the traditional CtA and UHV and some feasibility conditions are discovered.

A. Setup

The distributions of unexploited wind resource potential and ammonia industries in Inner Mongolia are shown in Figs. 4 and 5. Except for regions 1, 3, 5, 6, and 7, all other regions have available wind resources with FLH>4000 h, and the ammonia production concentrates in regions 1, 6 and 12. The topologies of the EN and HTN are also shown in Figs. 4 and 5. Detailed values of the economic indices are shown in the Nomenclature [9], [27], [37] and Table II. Values of c^{WC}, c^{HT}, EX^{EXP}, and EX^{UHV} are based on the real data in China. The parameters in (16) and (17) are listed in Fig. 9 and TableXIII in the Appendix.

B. Performance of the ADMM Algorithm

The original objective value in (15) is in the magnitude of 10^8, however, the extra items in the augmented Lagrangian in (45) is in the magnitude of 10^{10}, which would influence the quality of the optimal solution of the original problem. Therefore, a multiplier is required for EX^{WtA} in (46) and EX^{EN} in (47). Table III shows the convergence efficiency and the objective values with different multipliers.

Table III shows that if there is no extra multiplier or it is too small, the objective values are unreasonable because of the extra

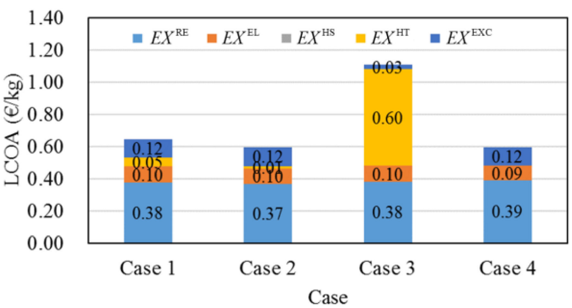

Fig. 7 Composition of LCOA in four cases.

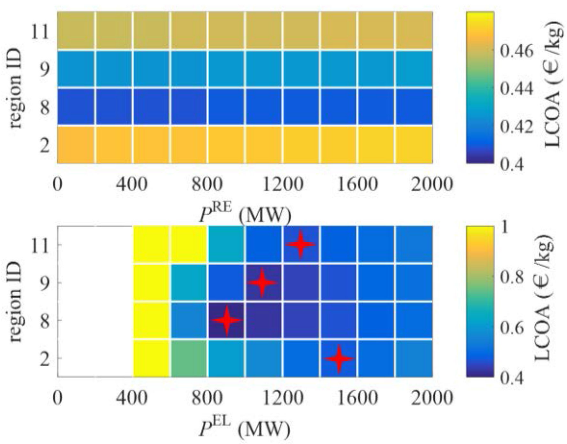

Fig. 8 Utilization cost of wind resources.

TABLE III
PERFORMANCE OF ADMM ALGORITHM FOR WTA-EN CO-PLANNING MODEL

Multiplier	Iteration times	EX^{WtA} (billion €)	EX^{EN} (billion €)
1	7	2.95	0.01
10	7	1.61	0.01
10^2	13	0.92	-0.03
10^3	55	0.76	-0.07
10^4	68	0.68	-0.12
10^5	583	0.68	-0.12

items in the augmented Lagrangian. However, when the multiplier is larger than 10^4, there is no obvious improvement on the optimal values, while the iteration times increase significantly. Therefore, 10^4 is the most suitable multiplier for this problem, which can ensure the quality of the optimal solution and the convergence efficiency at the same time.

C. Comparative Studies

Four comparative cases are studied in this section as follows:

1) Case 1: From the perspective of independent operators of the WtA and the EN, the WtA-EN co-planning problem in (15) is solved with the ADMM algorithm in Table I with exchanging limited information between the WtA operator and the EN operator.
2) Case 2: From the government's perspective who is supposed to own the overall information of both the WtA and the EN, the WtA-EN co-planning problem in (15) in the form of MIQCP (mixed-integer quadratically constrained programming) is directly solved based on CPLEX with branch and cut algorithm. Case 2 is set in comparison with Case 1 to analyze the different planning results based on the different algorithms.
3) Case 3: By limiting the locations of electrolyzers only in source regions, the EN is hence not necessarily expanded in this case. The extra constraint $P_{i,t}^{\mathrm{END}} \leq P_{i,t}^{\mathrm{A}}$ is added into the model (46), and the co-planning problem is solved with the ADMM algorithm. Case 3 is set in comparison with Case 1 to study the importance of power transmission via the EN, and the siting flexibility of PtA for the WtA planning.
4) Case 4: By limiting the locations of electrolyzers only in demand regions as comparison with Case 3, the hydrogen transport is hence not necessary in this case. The extra constraint $n_{i,t}^{\mathrm{HTS}} = 0$ is added into the model (46), and the co-planning problem is solved with the ADMM algorithm. Case 4 is set in comparison with Case 1 to study the importance of hydrogen transport via the HTN, and the siting flexibility of PtA for the EN expansion.

TABLE IV
OPTIMAL PLANNING RESULTS OF WTA (CASE 1 AND CASE 2)

Region	Case 1 P^{RE} (MW)	Case 1 P^{EL} (MW)	Case 1 m^{HS} (t)	Case 2 P^{RE} (MW)	Case 2 P^{EL} (MW)	Case 2 m^{HS} (t)
1		36			353	2
2	2088			1521		
6		1166	9		1085	3
8	713			757		
9		358			101	
11	1013			1424		
12	40	211	5	40	241	4
SUM	3854	1771	14	3742	1780	9

TABLE V
OPTIMAL EXPANSION RESULTS OF EN

	Case 1	Case 2
Line	5-17	1-8,1-14,3-4,5-6 6-10,12-15,14-15

1) Optimal Co-Planning Results of WtA-EN: Case 1: Table IV shows the optimal planning results of the WtA facilities. For P^{RE}, regions 2, 8, 11, and 12 have the planning wind turbines of 3854 MW in total, the capacity of region 12 has attained its maximal potential (40MW). For P^{EL}, the total capacity is 1771 MW, where 20% (358 MW) is located in the source regions (9), and 80% (1413 MW) is located in the demand regions (1, 6, 12). And then hydrogen produced in region 9 is transported to region 1 with the quantity of 112 t per day. For m^{HS}, 14 t buffer tanks which are no more than 3% of daily hydrogen demand (512 t) for ammonia synthesis are required in total in demand regions.

Table V shows the optimal planning results of EN transmission lines. Only one branch (5-17) is required to expand for power transmission.

2) Comparison with Case 2: The optimal planning results of WtA-EN of Case 2 are shown in Table IV and Table V. Compared with Case 1 with distributed planning, centralized planning in Case 2 results in the reduction of WtA capacity and the increase

TABLE VI
UTILIZATION RATE OF WIND GENERATION

Region	Case 1	Case 2	Case 3	Case 4
2	93%	97%	85%	89%
8	99%	98%	99%	92%
9			97%	
11	100%	100%		96%
12	99%	100%	100%	100%

TABLE VII
COST OF THE WTA OPERATOR AND THE EN OPERATOR (BILLION €)

Cost	Case 1	Case 2	Case 3	Case 4
EX^{WtA}	0.6830	0.6294	1.1559	0.6365
EX^{EN}	-0.1223	-0.1094	-0.0299	-0.0728
$EX^{\mathrm{WtA}}+EX^{\mathrm{EN}}$	0.5607	0.5200	1.1260	0.5637

TABLE VIII
OPTIMAL PLANNING RESULTS OF WTA (CASE 3 AND CASE 4)

Region	Case 3			Case 4		
	P^{RE} (MW)	P^{EL} (MW)	m^{HS} (t)	P^{RE} (MW)	P^{EL} (MW)	m^{HS} (t)
1					316	2
2	755	254		730		
6					1169	8
8	2362	1167		1197		
9	670	361				
11				1956		
12	40			40	164	3
SUM	3827	1782	0	3923	1649	13

on the EN expansion. In particular, 6 transmission lines are additionally expanded resulting in the capacity reduction of 110 MW (∼3%) wind turbines. Table VI shows the utilization rate of wind generation calculated by $\sum_{t=1}^{|\mathbb{T}|} P_{i,t}^{\mathrm{RE}}/(a_i P_i^{\mathrm{RE}^2}+b_i P_i^{\mathrm{RE}})$ according to the definition in (16) and (17), the numerator represents the utilized wind generation, and the denominator represents the maximal wind generation determined by P_i^{RE}. The co-planning of WtA-EN can reduce the wind energy spillage and improve the utilization rate of wind generation.

The economic analysis with two kinds of algorithms is shown in Table VII. Case 2 with centralized planning shows a lower total cost (−41 million EUR, 7%) with the larger expansion of the EN. However, it is not realistic for actual application since WtA and EN are generally operated independently. Case 1 considering independent operations of WtA and EN shows a better economy of the EN operator with the cost reduction of 13 million EUR, it is mainly because the sub-model of EN in (47) can take both the expansion cost EX^{EXP} and the operation income EX^{EXC} into consideration, which helps the EN operator make a better expansion decision.

Table VI and Table VII also show that the co-planning of WtA-EN is better than Case 3 (without EN expansion) and Case 4 (without location planning of electrolyzers), which verifies the advantage of the co-planning of WtA-EN on facilitating wind power utilization and reducing total investment costs.

3) Comparison with Case 3 and Case 4: The optimal planning results of Case 3 and Case 4 are shown in Table VIII. Case 3 studies the optimal planning of WtA-EN without EN expansion, and Case 4 studies the optimal planning of WtA-EN without hydrogen transport.

As shown in Table VII, in Case 3, the cost of the WtA operator EX^{WtA} sees a significant increase (+473 million EUR), and the total economy of $EX^{\mathrm{WtA}}+EX^{\mathrm{EN}}$ (+565 million EUR, 101%) also gets worse compared with Case 1. It is mainly due to the expensive hydrogen transport cost via HT. After all, compared with the wheeling fee of 0.008 €/kWh (∼0.44 €/kg) via the EN, the transportation cost of 1 €/100km/kg via HT is uneconomic (H_2 pipelines are not considered). It verifies the value of power transmission and the expansion of branch 5-17 in Case 1, and reveals the benefit of the siting flexibility of PtA for the WtA planning.

In Case 4, Table VII shows that the investment cost of the EN operator EX^{EN} increases significantly (+50 million EUR) with extra investments on 15 extra transmission lines, and the total economy of $EX^{\mathrm{WtA}}+EX^{\mathrm{EN}}$ (+3 million EUR, 0.5%) also gets worse compared with Case 1. It verifies the necessity of hydrogen transport from region 9 to region 1 in Case 1, and reveals the benefit of the siting flexibility of PtA for the EN expansion.

In summary, comparative case studies verify the importance of PtA with siting and operation flexibility brought by HSC for both WtA and EN planning. Especially for the EN operator, PtA with HSC can significantly reduce the burden on the EN expansion.

4) Economic Analysis: From the perspective of the WtA operator, Fig. 7 shows the compositions of LCOAs in the above analyzed four cases. The LCOA is 0.65 €/kg in Case 1. In general, EX^{RE} and EX^{EL} are the most important parts, which account for 58% and 15% of the LCOA, respectively. EX^{HS} is minor compared with other components. There are significant differences in EX^{HT} and EX^{EXC} among the different cases. In Case 2, EX^{HT} only contributes to 0.01 €/kg for LCOA, while in Case 1, EX^{HT} contributes to around 0.05 €/kg. However, in Case 3, without power transmission via EN, it shows an extremely high cost via HT (0.60 €/kg) as hydrogen truck does not represent the best option for long-distance hydrogen transport.

On the contrary, from the perspective of the EN operator, based on EX^{EXP}, the levelized cost of the expansion for power transmission expressed as $\sum_{ij\in\mathbb{B}} EX_{ij}^{\mathrm{EXP}}/\sum_{i\in\mathbb{R}}\sum_{t=1}^{|\mathbb{T}|}\widehat{P}_{i,t}^{\mathrm{END}}$ can be obtained, which are 0.0073, 0.0888, 0.3248 € cents/kWh in Case 1, Case 2, Case 4, respectively. It is uneconomic for the EN operator to expand transmission lines to afford all the required energy transmission, which verifies the advantage of the co-planning of WtA-EN in balancing the utilization rate of facilities from the macro-perspective.

The following discussions are all based on the proposed WtA-EN co-planning model with distributed ADMM algorithm.

D. Key Factors Related to the Siting and Sizing of WtA

In this subsection, four key factors related to the siting and sizing of WtA are summarized in Table IX.

TABLE IX
FACTORS RELATED TO THE SITING AND SIZING DECISIONS

		Wind resources	Ammonia demands	Facility costs	Energy transport modes
Siting	WT	√			
	EL				√
	HS		√		
Sizing	WtA	√	√	√	√

Notice that the optimal WtA siting results in Table IV and Table VIII do not include eastern regions 4, 5, 7, 10 shown in Figs. 4 and 5. It is because the western 8 regions and the eastern 4 regions belong to different operators in Inner Mongolia, so the two networks are physically disconnected, as shown in Fig. 4. This situation has been modeled by the node-branch associate matrix $\mathbf{T}_{\mathrm{E}}$ in (34). Besides, the ammonia industries gather in the western regions 1, 6, and 12. The long distance transportations are hence uneconomic from the eastern regions to the western regions, as shown in Fig. 7. Therefore, the wind turbines concentrate in the source regions (2, 8, 9, 11, 12), and the hydrogen buffer tanks are located in the demand regions (1, 6, 12) next to the ammonia synthesis reactors. The siting of electrolyzers depends on energy transport modes, with power transmission corresponding to demand regions-sited and hydrogen transport corresponding to source regions-sited.

The sizing of WtA is naturally related to the total ammonia demands. The other three key factors in Table IX on the sizing of WtA facilities are discussed as follows.

1) Wind Resources: To study the influences of the indices of wind resources (FLH and variability defined in Section III) on the sizing of the WtA facilities, in this subsection, the utilization cost of wind resources LCOA in each region is quantitatively calculated. The results are shown in Fig. 8.

The upper figure in Fig. 8 shows the calculation results of the LCOA based on the same model and the algorithm as Case 1 with different P^{RE} in different regions. In each region, the LCOA increases with P^{RE} increasing, which is due to the declining tendency of the average FLH. Different regions indicate different changing tendencies. For example, with the increasing of P^{RE} from 0 to 2000 MW, the LCOA increases 0.005 €/kg in region 2 while only 0.001 €/kg in region 8.

Furthermore, for the same P^{RE}, LCOAs are different with different P^{EL}. Take $P^{\mathrm{RE}}=$ 2000MW as an example, the results are shown in the lower figure in Fig. 8. For each region, there is an optimal P^{EL} marked with the red star in Fig. 8 corresponding to the minimum LCOA. The optimal ratios of P^{EL} to P^{RE} are around 80%, 50%, 60%, 70% in region 2, 8, 9, 11, respectively. That can be explained by the different wind power variabilities in each region, as shown in Fig. 9 in the Appendix.

2) Energy Transport Modes: Compared Case 1 with Cases 3 and 4 in Table IV and Table VIII, as the energy transport modes gradually convert from hydrogen-majored to power-majored (from Case 3 to Case 1, to Case 4), the capacity of P^{EL} and the ratio of P^{EL} to P^{RE} gradually decrease (from 47% to 46%, to 42%). This phenomenon reveals that power transmission via the EN would help to eliminate the fluctuation of wind generation, which leads to the reduction of the optimal capacity of electrolyzers. The sizing of hydrogen buffer tanks is also related to energy transport modes since HT can be treated as a mobile supplement for the hydrogen storage of buffer tanks. Hence, HS's capacity in Case 3 is the least.

3) Facility Costs: Furthermore, the sizing of wind turbines and electrolyzers is also related to facility costs. This is discussed in the next subsection.

E. Analysis on Feasibility Conditions of WtA

Wind resources-based ammonia is a new kind of pathway for both renewable energy utilization and the ammonia industry. In particular, traditional ammonia industry is coal-based in Inner Mongolia, and traditional renewable energy utilization in Inner Mongolia is UHV-based. In this section, WtA is compared with CtA and UHV to obtain the feasibility conditions of this mode.

1) Comparison with CtA: The average LCOA for WtA in Inner Mongolia is 0.65 €/kg, while the average LCOA for CtA considering the carbon tax of approximately 25 €/t [40] is only 0.41 €/kg [41]. According to Fig. 7, the higher cost for green ammonia is mainly due to the relatively expensive capacity cost of wind turbines (1000 €/kW) and electrolyzers (375 €/kW) which contribute to 58% and 15% of LCOA, respectively. To attain a competitive cost of WtA, the decline of the facility costs in the future or the subsidy at present is required to initialize the WtA market and support for the substitution of WtA to CtA. As the difference between the two costs is 0.24 €/kg and according to the composition of LCOA in Fig. 7, here are three potential subsidy types discussed:

1) Subsidy for wind turbines. With the subsidy of 632 €/kW for wind turbines, LCOA for WtA can reduce to 0.41 €/kg.
2) Subsidy for electrolyzers and wind turbines with the higher priority of electrolyzers. With the subsidy of 375 €/kW for electrolyzers, LCOA for WtA can reduce to 0.55 €/kg first, and a subsidy of 368 €/kW for wind turbines is still required for the remaining difference.
3) Subsidy for wind turbines and electrolyzers with the same ratio. With the subsidy of 500 €/kW for wind turbines and 187.5 €/kW for electrolyzers, LCOA for WtA can reduce to 0.41 €/kg.

The above subsidy types are just the basic analysis based on the planning results of Case1. Actually, different subsidy types lead to different optimal planning results, and also different total subsidy for the involved operators. Based on the proposed WtA-EN co-planning model, the actual LCOA and total subsidy of the above three types are shown in Table X below:

From Table X, following conclusions can be drawn:

1) Compared with the planning results of Case 1 with $P^{\mathrm{RE}}=$ 3854MW and $P^{\mathrm{EL}}=$ 1771MW, with the decline of c^{RE} in subsidy type 1, the ratio of P^{EL} to P^{RE} decreases from 46% to 39%; with the decline of c^{EL} in subsidy type 2, the ratio of P^{EL} to P^{RE} increases from 46% to 48%. The influence of the facility costs on the sizing of P^{RE} and P^{EL} reveals that the cheaper facility with the larger capacity is required to ensure the utilization rate of the expensive one.

TABLE X
PERFORMANCE OF DIFFERENT SUBSIDY TYPES

Type	LCOA (€/kg)	P^{RE} (MW)	P^{EL} (MW)	Subsidy (billion €)	EX^{WtA} (billion €)	EX^{EN} (billion €)
1	0.3999	4210	1624	2.66	0.4238 (-0.2592)	-0.1226 (-0.0003)
2	0.4075	3856	1861	2.12	0.4322 (-0.2508)	-0.1224 (-0.0001)
3	0.4063	3961	1738	2.31	0.4307 (-0.2523)	-0.1225 (-0.0002)

TABLE XI
LEVELIZED COST OF UHV

Utilization rate of wind generation	Type of UHV	E (TWh)	LCOU (€/kWh)
100%	1	41.84	0.0060
80%	2	21.96	0.0069
60%	3	14.73	0.0082

2) Actual LCOAs with all three subsidy types are below 0.41 €/kg with the better planning results than Case 1. However, with the subsidy for c^{RE} decreasing and that for c^{EL} increasing (from subsidy type 1 to 3, to 2), LCOA increases slightly with the obvious reduction on the total subsidy (0.54 billion euros can be saved), which reveals that the subsidy priority of c^{EL} should be higher than c^{RE} since the total capacity of P^{EL} is less.
3) Calculation results on the annual cost of the WtA operator and the EN operator shown in Table X reveal that both operators can benefit from the subsidy. Especially for the WtA operator, the annual cost EX^{WtA} decreases by over 35% since the subsidy is direct for facility costs of wind turbines or electrolyzers.

Furthermore, according to the ammonia production in Inner Mongolia (1.06 Mt), the substitution of WtA to CtA can save approximately 1.79 Mtce of coal consumption [42] and reduce up to 4.89 Mt of CO_2 emission [43] per year, which is also one major advantage of WtA.

2) Comparison with UHV: In this section, the comparative economic analysis of power delivered by UHV transmission lines and WtA is studied. Due to the spatial discrepancy of renewable energy and electric demand, the State Grid Corporation of China has established several UHV transmission lines to achieve long-distance and large-scale power transmission [44]. We compare these two kinds of methods for future renewable energy utilization. Economic calculation is referred to the existing UHV project from Shanghaimiao in Inner Mongolia to Linyi in Shandong with a total length of 1230km of UHV transmission line [44], and we consider an unexplored 10GW wind farm in Inner Mongolia for example. In this way the levelized cost of UHV (LCOU) can be calculated based on economic parameters shown in Table II and the evaluation results of wind resources. Here we consider three types of UHV transmission lines.

Table XI shows that in this case, the most economical type is type 1, and the corresponding LCOU $= 0.0060$ €/kWh. It should be noticed that the profit of UHV mode stems from the differences in LCOEs between source regions and demand regions, and the profit of WtA results from the differences between LCOAs for WtA and for CtA.

TABLE XII
ECONOMIC COMPARISON OF UHV WITH WTA

Reduction percentage on WT costs	UHV (€/kWh)	WtA (€/kWh)
100%	-0.004	-0.046
75%	-0.005	-0.027
50%	-0.007	-0.008

According to the evaluation of wind resources in Shandong (SD) Province, the average LCOE$^{\mathrm{SD}}$ $= 0.0364$ €/kWh. And in Inner Mongolia (IM), we choose LCOE$^{\mathrm{IM}}$ $= 0.0337$ €/kWh in region 8. Therefore the unit profit per kWh for UHV mode can be expressed as LCOE$^{\mathrm{SD}}$-LCOE$^{\mathrm{IM}}$-LCOU, and the unit profit per kWh for WtA mode can be expressed as (LCOA$^{\mathrm{WtA}}$-LCOA$^{\mathrm{CtA}}$)/LHV$_{\mathrm{NH_3}}$, where LHV$_{\mathrm{NH_3}}$$=5.2$ kWh/kg is the lower heating value of ammonia [7]. Furthermore, similar to the analysis above, the unit profit per kWh for both modes can be calculated, and the results are shown in Table XII.

Table XII shows that the economy of UHV mode will get worse with the decline of the facility cost. On the contrary, the economy of WtA mode will get better. A reduction of 60% in c^{RE} (when $c^{\mathrm{RE}}$$= 400$ €/kW) in the future will lead to profits for WtA mode. It reveals that there is potential complementarity of UHV and WtA in the long planning horizon under the decline tendency of facility costs.

V. CONCLUSION

This paper proposes the generic configuration of regional WtA-EN. From the perspective of power systems, the power load model of PtA with HSC is first proposed with both siting flexibility and operation flexibility. On this basis, the co-planning model of WtA and EN is proposed to minimize the total infrastructure investments. The cases based on the real data of Inner Mongolia in China are studied, and the conclusions can be drawn as follows:

1) The flexibilities of PtA with HSC is beneficial to both WtA and EN planning. Especially for the EN operator, the optimized siting strategies of PtA with the supplement of hydrogen transport can reduce the burden on the EN expansion.
2) The co-planning of WtA and EN not only enhances the utilization of wind generation but also reduces the total cost, which is helpful for the deployment of WtA.
3) Wind resources, ammonia demands, facility costs, and energy transport modes are the four key factors related to the siting and sizing of WtA. In particular, the utilization cost of wind resources is determined by both FLH and variability: the former index decides the LCOE, and the latter index decides the LCOA with an optimal capacity ratio of electrolyzers over wind turbines. This ratio is also strongly related to facility costs and energy transport modes.
4) For the substitution to CtA, at present, the subsidy is required to initialize the WtA market, the minimum total subsidy of 2 billion euros (near 50% of the total investment

costs of WtA) is required with the optimal subsidy type for electrolyzers first. To compete with UHV, the cost reduction of over 50% on wind turbines would enable the feasibility of WtA.

APPENDIX

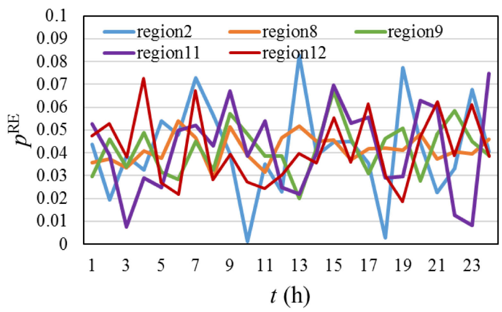

Fig. 9. The variable profiles of wind power.

TABLE XIII
PARAMETERS IN (16) AND (17)

Region	a_i (h/d/MW)	b_i (h/d)	$P_i^{RE,max}$ (MW)
2	-1.39e-05	11.52	22585
4	-1.58e-04	12.52	980
8	-6.34e-05	11.44	2655
9	-3.81e-05	11.50	2240
10	-7.02e-04	12.66	250
11	-3.36e-05	11.58	6820
12	-5.49e-02	13.99	40

REFERENCES

[1] C. M. Administration, “2018 Annual bulletin of wind and solar energy resources,” 2019. [Online]. Available: http://www.cma.gov.cn/2011xwzx/2011xqxxw/2011xqxyw/201901/t20190123_513192.html
[2] W. Liu, H. Lund, B. V. Mathiesen, and X. Zhang, “Potential of renewable energy systems in china,” *Appl. Energy*, vol. 88, no. 2, pp. 518–525, 2011.
[3] S. Yu, Y. Zheng, and L. Li, “A comprehensive evaluation of the development and utilization of china’s regional renewable energy,” *Energy Policy*, vol. 127, pp. 73–86, 2019.
[4] National Energy Administration, “National power industry statistics in 2019,” 2020. [Online]. Available: http://www.nea.gov.cn/2020-01/20/c_138720881.htm
[5] M. J. Palys, H. Wang, Q. Zhang, and P. Daoutidis, “Renewable ammonia for sustainable energy and agriculture: Vision and systems engineering opportunities,” *Curr. Opin. Chem. Eng.*, vol. 31, 2021, Art. no. 100667.
[6] L. Zhang *et al.*, “Driving factors and predictions of CO2 emission in china’s coal chemical industry,” *J. Clean. Prod.*, vol. 210, no. 2019, pp. 1131–1140, 2019.
[7] A. Valera-Medina, H. Xiao, M. Owen-Jones, W. I. F. David, and P. J. Bowen, “Ammonia for power,” *Prog. Energy Combust. Sci.*, vol. 69, pp. 63–102, 2018.
[8] A. Allman, and P. Daoutidis,“Optimal scheduling for wind-powered ammonia generation: Effects of key design parameters,” *Chem. Eng. Res. Des.*, vol. 131, pp. 5–15, 2018.
[9] J. Li, J. Lin, and Y. Song, “Capacity optimization of hydrogen buffer tanks in renewable power to ammonia (P2A) system,” in *Proc. IEEE Power Energy Soc. Gen. Meeting*, Montreal, QC, Canada, 2020, pp. 1–5.
[10] J. Armijo, and C. Philibert, “Flexible production of green hydrogen and ammonia from variable solar and wind resources: Case study of chile and argentina,” *Int. J. Hydrogen Energy*, vol. 45, no. 3, pp. 1541–1558, 2020.
[11] V. Kyriakou, I. Garagounis, E. Vasileiou, A. Vourros, and M. Stoukides, “Progress in the electrochemical synthesis of ammonia,” *Catalysis Today*, vol. 286, pp. 2–13, 2017.
[12] D. Xu *et al.*, “Integrated modelling and enhanced utilization of power-to-ammonia for high renewable penetrated multi-energy systems,” *IEEE Trans. Power Syst.*, vol. 35, no. 6, pp. 4769–4780, Nov. 2020.
[13] A. Sánchez and M. Martín, “Optimal renewable production of ammonia from water and air,” *J. Cleaner Prod.*, vol. 178, pp. 325–342, 2018.
[14] D. Frattini, G. Cinti, G. Bidini, U. Desideri, R. Cioffi, and E. Jannelli, “A system approach in energy evaluation of different renewable energies sources integration in ammonia production plants,” *Renewable Energy*, vol. 99, pp. 472–482, 2016.
[15] O. Siddiqui, and I. Dincer, “Optimization of a new renewable energy system for producing electricity, hydrogen and ammonia,” *Sustain. Energy Technol. Assessments*, vol. 44, 2021, Art. no. 101023.
[16] A. Hasan, and I. Dincer, “Development of an integrated wind and PV system for ammonia and power production for a sustainable community,” *J. Clean. Prod.*, vol. 231, pp. 1515–1525, 2019.
[17] K. Verleysen, D. Coppitters, A. Parente, W. De Paepe, and F. Contino, “How can power-to-ammonia be robust? Optimization of an ammonia synthesis plant powered by a wind turbine considering operational uncertainties,” *Fuel*, vol. 266, 2020, Art. no. 117049.
[18] J. Ikäheimo, J. Kiviluoma, R. Weiss, and H. Holttinen, “Power-to-ammonia in future north european 100% renewable power and heat system,” *Int. J. Hydrogen Energy*, vol. 43, no. 36, pp. 17295–17308, 2018.
[19] S. Schulte Beerbühl, M. Fröhling, and F. Schultmann, “Combined scheduling and capacity planning of electricity-based ammonia production to integrate renewable energies,” *Eur. J. Oper. Res.*, vol. 241, no. 3, pp. 851–862, 2015.
[20] A. Allman, and P. Daoutidis, “Ammonia supply chains: A new framework for renewable generation with a case study for minnesota,” *Comput. Chem. Eng.*, vol. 38, pp. 1395–1400, 2016.
[21] A. Allman, P. Daoutidis, and D. Tiffany, “A framework for ammonia supply chain optimization incorporating conventional and renewable generation,” *AIChE J.*, vol. 63, pp. 4390–4402, 2017.
[22] H. Dagdougu, “Models, methods and approaches for the planning and design of the future hydrogen supply chain,” *Int. J. Hydrogen Energy*, vol. 37, no. 6, pp. 5318–5327, Mar. 2012.
[23] National Energy Administration, “Operation statistics of wind power in 2019,” 2020. [Online]. Available: http://www.nea.gov.cn/2020-02/28/c_138827910.htm
[24] D. S. Ryberg, Z. Tulemat, D. Stolten, and M. Robinius, “Uniformly constrained land eligibility for onshore european wind power,” *Renewable Energy*, vol. 146, pp. 921–931, 2020.
[25] D. S. Ryberg, M. Robinius, and D. Stolten, “Evaluating land eligibility constraints of renewable energy sources in europe,” *Energies*, vol. 11, no. 1246, pp. 1–19, 2018.
[26] Inner Mongolia Autonomous Regional Bureau of Statistics, “Statistical yearbook of inner mongolia in 2019,” 2020. [Online]. Available: http://tj.nmg.gov.cn/Files/tjnj/2019/zk/indexch.htm
[27] J. Li *et al.*, “Optimal investment of electrolyzers and seasonal storages in hydrogen supply chains incorporated with renewable electric networks,” *IEEE Trans. Sustain. Energy*, vol. 11, no. 3, pp. 1773–1784, Jul. 2020.
[28] G. Pan, W. Gu, Y. Lu, H. Qiu, S. Lu, and S. Yao, “Optimal planning for electricity-hydrogen integrated energy system considering power to hydrogen and heat and seasonal storage,” *IEEE Trans. Sustain. Energy*, vol. 11, no. 4, pp. 2662–2676, Oct. 2020.
[29] S. Samsatli, and N. J. Samsatli, “A general spatiotemporal model of energy systems with a detailed account of transport and storage,” *Comput. Chem. Eng.*, vol. 80, no. 2, pp. 155–176, 2015.
[30] M. M. Benito, P. Agnolucci, and L. G. Papageorgiou, “Towards a sustainable hydrogen economy: Optimisation-based framework for hydrogen infrastructure development,” *Comput. Chem. Eng.*, vol. 102, pp. 110–127, Jul. 2017.
[31] P. Nunes, F. Oliveira, S. Hamacher, and A. Almansoori, “Design of a hydrogen supply chain with uncertainty,” *Int. J. Hydrogen Energy*, vol. 40, no. 46, pp. 16408–16418, Dec. 2015.
[32] P. M. Heuser, D. S. Ryberg, T. Grube, M. Robinius, and D. Stolten, “Techno-economic analysis of a potential energy trading link between patagonia and japan based on CO2 free hydrogen,” *Int. J. Hydrogen Energy*, vol. 44, no. 25, pp. 12733–12747, 2019.
[33] X. Zhang, and A. J. Conejo, “Coordinated investment in transmission and storage systems representing long and short-term uncertainty,” *IEEE Trans. Power Syst.*, vol. 33, no. 6, pp. 7143–7151, Nov. 2018.
[34] L. Bahiense, G. C. Oliveira, M. Pereira, and S. Granville, “A mixed integer disjunctive model for transmission network expansion,” *IEEE Trans. Power Syst.*, vol. 16, no. 3, pp. 560–565, Aug. 2001.
[35] Y. Nie, M. Farrokhifar, and D. Pozo, “Electricity and gas network expansion planning: An the ADMM-based decomposition approach,” in *Proc. IEEE Milan PowerTech*, Milan, Italy, 2019, pp. 1–6.

[36] S. Boyd, N. Parikh, E. Chu, B. Peleato, and J. Eckstein, "Distributed optimization and statistical learning via the alternating direction method of multipliers," *Foundations Trends Mach. Learn.*, vol. 3, no. 1, pp. 1–122, Jul. 2011.

[37] J. Koponen, "Review of water electrolysis technologies and design of renewable hydrogen production systems," *Lappeenranta University of Technology*, 2015.

[38] M. Reuß, T. Grube, M. Robinius, and D. Stolten, "A hydrogen supply chain with spatial resolution: Comparative analysis of infrastructure technologies in germany," *Appl. Energy*, vol. 247, pp. 438–453, 2019.

[39] M. Reuß, T. Grube, M. Robinius, P. Preuster, P. Wasserscheid, and D. Stolten, "Seasonal storage and alternative carriers: A flexible hydrogen supply chain model," *Appl. Energy*, vol. 200, pp. 290–302, 2017.

[40] D. R. MacFarlane *et al.*, "A roadmap to the ammonia economy," *Joule*, 2020.

[41] OILCHEM, "Ammonia price data," 2020. [Online]. Available: https://dc.oilchem.net/price_search

[42] W. Zhou, B. Zhu, Q. Li, T. Ma, S. Hu, and C. Griffy-Brown, "CO2 emissions and mitigation potential in china's ammonia industry," *Energy Policy*, vol. 38, no. 7, pp. 3701–3709, 2010.

[43] Y. Zhang *et al.*, "Intensive carbon dioxide emission of coal chemical industry in china," *Appl. Energy*, vol. 236, pp. 540–550, 2019.

[44] State Grid Corporation, "UHV projects," [Online]. Available: http://www.sgcc.com.cn/html/sgcc_main/col2017041259/column_2017041259_1.shtml?childColumnId=2017041259

Jiarong Li was born in November 1995. She received the B.S. degree from Xi'an Jiaotong University, Xi'an, China, in 2016. She is currently working toward the Ph.D. degree with the Department of Electrical Engineering, Tsinghua University, Beijing, China. She is currently a Research Assistant with Smart Grid Operation and Optimization Laboratory. Her research interests include planning and optimization of the P2X energy system.

Jin Lin (Member, IEEE) was born in 1985. He received the B.S. and Ph.D. degrees in electrical engineering from Tsinghua University, Beijing, China, in 2007 and 2012, respectively. He is currently an Associate Professor and Doctoral Supervisor with the Department of Electrical Engineering, Tsinghua University, and the Director of the Smart Hydrogen Energy Laboratory, Tsinghua Sichuan Energy Internet Research Institute. He has authored or coauthored more than 80 SCI/EI papers. His main research interests over the years include the fields of high-temperature electricity hydrogen production, electro-hydrogen coupling systems, and smart hydrogen energy. He is mainly engaged in the research of high temperature electric hydrogen production, electric hydrogen coupling system, and smart hydrogen energy. He was the recipient of the award for the Thousand Talents Plan Program of Sichuan Province in 2017. He was also the recipient of the Young Chang Jiang Scholars Program by the Ministry of Education and Beijing New Star Program of Science and Technology. He is currently the Secretary-General of the National Hydrogen Standards Committee Renewable Energy Hydrogen Standard Working Group, Secretary-General of the Hydrogen Energy System Special Committee of the International Hydrogen Energy Association, Deputy Secretary-General of the Hydrogen Energy Special Committee of IEEE China, and Secretary-General of the Smart Hydrogen Special Committee of the National Energy Internet Alliance, Member of CIGRE Hydrogen Energy Working Group. He has participated in a number of key research projects supported by a variety funding bodies, including the National Natural Science Foundation of China, National Key Research and Development Program of China, Chinese National Programs for High Technology Research and Development (863 Program), and National Program on Key Basic Research Project (973 Program).

Philipp-Matthias Heuser received the graduation degree and the master's degree in mechanical engineering and management, business and economics from RWTH Aachen University, Aachen, Germany. He is elaborating the integration of hydrogen into the energy system and energy markets. As a Senior Consultant with E-Bridge Consulting, his work focuses on the development of gas markets and transport networks, sector coupling, and regulatory analysis for the implementation of the national hydrogen strategy. Furthermore, he supports national and international projects in project management. He gained expertise and experience in this field during his doctoral studies at the Institute for Energy and Climate Research of the Research Center Jülich, where he designed a concept for a worldwide hydrogen infrastructure based on renewable energy.

Heidi Ursula Heinrichs received the Diploma in mechanical engineering from RWTH Aachen University, Aachen, Germany, and the Ph.D. degree in engineering from the Karlsruhe Institute of Technology, Karlsruhe, Germany. She heads the group Energy Potentials and Supply Pathways with the Institute for Techno-Economic Systems Analysis, Juelich Research Center, Germany. Her research and teaching interests include energy scenarios, modeling pathways towards sustainable energy systems, and integrating social, economic and technical dimensions in energy systems analysis, recently with a special focus on the global scale and green hydrogen. She works in these fields in Jülich, Cambridge and Karlsruhe.

Jinyu Xiao was born in 1977. He received the B.S. and Ph.D. degrees in electrical engineering from Tsinghua University, Beijing, China, in 2000 and 2005, respectively. He is currently a Professor-level Senior Engineer with Global Energy Interconnection Development and Cooperation Organization. His research interests include renewable generation integration, green hydrogen supply chain, and stability characteristics of high penetration renewable energy power system.

Feng Liu (Senior Member, IEEE) received the B.Sc. and Ph.D. degrees in electrical engineering from Tsinghua University, Beijing, China, in 1999 and 2004, respectively. He is currently an Associate Professor with Tsinghua University. From 2015 to 2016, he was a Visiting Associate with California Institute of Technology, Pasadena, CA, USA. He is the author or coauthor of more than 200 peer-reviewed technical papers and two books, and holds more than 20 issued or pending patents. His research interests include stability analysis, optimal control, robust dispatch, and game theory based decision making in energy and power systems. He is an Associated Editor of several international journals, including the IEEE TRANSACTIONS ON SMART GRID and IEEE PES Letter. He was also a Guest Editor of the IEEE TRANSACTIONS ON ENERGY CONVERSION.

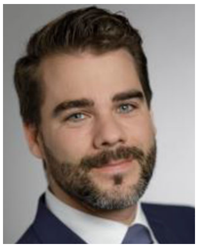

Martin Robinius received the Bachelor of Engineering degree from the University of Applied Sciences and Arts, Hannover, Germany, the Master of Science degree from Kassel University, Kassel, Germany, and the D.Eng. degree from RWTH Aachen University, Aachen, Germany. He is currently the Head of energy policy and energy systems with umlaut SE, Aachen. Umlaut SE is an independent, globally operating management consultancy providing management and engineering services. The company has an annual turnover of more than 400 million euros and employs about 4500 people worldwide. Prior to taking up his current position, he was the Deputy Director of the Techno-Energy Systems Modeling Institute, Forschungszentrum Jülich, Germany. His task was leading approximately 40 researchers, doctoral candidates, master's and bachelor's students who perform research for techno-economic energy system modeling, analysis and assessment. He wrote his PhD thesis at the same institute, and for which he won several awards. During that time, he was also a Visiting Researcher with National Renewable Energy Laboratory, USA. He began his career with the Fraunhofer Institute for Wind Energy and Energy System Technology. He also worked for a strategic consulting firm in China on a country analysis and site selection project in Asia and at Shanghai Volkswagen. He was a part of the Board of Directors of the Gesellschaft für Energiewissenschaft und Energiepolitik e. V., the German section of the International Association for Energy Economics, subtopic leader for the International Energy Agency and an independent consultant for private and public sectors. He has authored more than 60 publications in journals, such as *Applied Energy*, *Energies*, *International Journal of Hydrogen Energy*, and *Renewable Energy* and has been cited more than 3.000 times. His research interests include techno-economic energy systems assessment and modeling of power and gas transmission and distribution systems.

Yonghua Song (Fellow, IEEE) received the B.E. degree in electrical engineering from the Chengdu University of Science and Technology, Chengdu, China, in 1984 and the Ph.D. degree in electrical engineering from the China Electric Power Research Institute, Beijing, China, in 1989. He was awarded D.Sc. by Brunel University, Uxbridge, U.K., in 2002, Honorary DEng by University of Bath, Bath, U.K., in 2014 and Honorary D.Sc. by University of Edinburgh, Edinburgh, U.K., in 2019. From 1989 to 1991, he was a Postdoctoral Fellow with Tsinghua University, Beijing, China. He then held various positions with Bristol University, Bristol, U.K., Bath University, and John Moores University, Liverpool, U.K., from 1991 to 1996. In 1997, he was a Professor of power systems with Brunel University, where he was a Pro-Vice Chancellor for Graduate Studies since 2004. In 2007, he took up a Pro-Vice Chancellorship and Professorship of electrical engineering with the University of Liverpool, Liverpool, U.K. In 2009, he joined Tsinghua University, as a Professor of electrical engineering and an Assistant President and the Deputy Director of the Laboratory of Low-Carbon Energy. During 2012–2017, he was the Executive Vice President of Zhejiang University, Hangzhou, China, the Founding Dean of the International Campus, and a Professor of electrical engineering and Higher Education of the University. Since 2018, he has been a Rector of the University of Macau, Zhuhai, China, and the Director of the State Key Laboratory of Internet of Things for Smart City. His current research interests include smart grid, electricity economics, and operation and control of power systems. He was elected as the Vice-President of Chinese Society for Electrical Engineering (CSEE) and appointed as the Chairman of the International Affairs Committee of the CSEE in 2009. In 2004, he was elected as a Fellow of the Royal Academy of Engineering, U.K. In 2019, he was elected as a Foreign Member of the Academia Europaea.

Detlef Stolten is the Director of the Institute of Techno-Economic Systems Analysis (IEK-3), Juelich Research Center, Germany and since 2000, he has been holding the Chair for fuel cells with the RWTH Aachen University, Aachen, Germany. His research interests include electrochemistry and process engineering for different types of fuel cells and electrolyzers. Energy systems analysis and energy strategy form a new research topic taken up in 2010. It focuses on interconnecting the energy sectors and the role of storage encompassing gas and electric grid modeling, renewable power input, transportation energy requirements and storage via hydrogen, methane, LOHC and other options including renewable hydrogen production via electrolysis. For 12 years, he worked in the industry with Bosch and Daimler Benz/Dornier.